Higher metastatic efficiency of KRas G12V than KRas G13D in a colorectal cancer model

Patricia Alamo,[*,†] Alberto Gallardo,[†,‡] Federica Di Nicolantonio,[§,¶] Miguel Angel Pavón,[*,†] Isolda Casanova,[*,†] Manuel Trias,[†,‖] María Antonia Mangues,[#] Antonio Lopez-Pousa,[†,] Antonio Villaverde,[†,††] Esther Vázquez,[†,††] Alberto Bardelli,[§,¶,‡‡,§§] María Virtudes Céspedes,[*,†,1] and Ramón Mangues[*,†,1,2]**

*Oncogenesis and Antitumor Drug Group, Biomedical Research Institute Sant Pau, Hospital de la Santa Creu i Sant Pau, Barcelona, Spain; [†]CIBER de Bioingeniería, Biomateriales y Nanomedicina, Barcelona, Spain; [‡]Department of Pathology, Clínica Girona, Girona, Spain; [§]Department of Oncology, University of Torino, Torino, Italy; [¶]Candiolo Cancer Institute–Fondazione del Piemonte per l'Oncologia, Istituto Di Ricovero e Cura a Carattere Scientifico, Torino, Italy; Departments of [‖]General and Digestive Surgery, [#]Pharmacy, and **Medical Oncology, Hospital de la Santa Creu i Sant Pau, Barcelona, Spain; [††]Institut de Biotecnologia i de Biomedicina, and [‡‡]Department de Genètica i de Microbiologia, Universitat Autònoma de Barcelona, Barcelona, Spain; and [§§]FIRC Institute of Molecular Oncology, Milan, Italy

ABSTRACT **Although all KRas (protein that in humans is encoded by the *KRas* gene) point mutants are considered to have a similar prognostic capacity, their transformation and tumorigenic capacities vary widely. We compared the metastatic efficiency of KRas G12V (Kirsten rat sarcoma viral oncogene homolog with valine mutation at codon 12) and KRas G13D (Kirsten rat sarcoma viral oncogene homolog with aspartic mutation at codon 13) oncogenes in an orthotopic colorectal cancer (CRC) model. Following subcutaneous preconditioning, recombinant clones of the SW48 CRC cell line [Kras wild-type (Kras WT)] expressing the KRas G12V or KRas G13D allele were microinjected in the mouse cecum. The percentage of animals developing lymph node metastasis was higher in KRas G12V than in KRas G13D mice. Microscopic, macroscopic, and visible lymphatic foci were 1.5- to 3.0-fold larger in KRas G12V than in KRas G13D mice ($P < 0.05$). In the lung, only microfoci were developed in both groups. KRas G12V primary tumors had lower apoptosis (7.0 ± 1.2 *vs.* 7.4 ± 1.0 per field, $P = 0.02$), higher tumor budding at the invasion front (1.2 ± 0.2 *vs.* 0.6 ± 0.1, $P = 0.04$), and a higher percentage of C-X-C chemokine receptor type 4 (CXCR4)-overexpressing intravasated tumor emboli (49.8 ± 9.4% *vs.* 12.8 ± 4.4%, $P < 0.001$) than KRas G13D tumors. KRas G12V primary tumors showed Akt activation, and β5 integrin, vascular endothelial growth factor A (VEGFA), and Serpine-1 overexpression, whereas KRas G13D tumors showed integrin β1 and angiopoietin 2 (Angpt2) overexpression. The increased cell survival, invasion, intravasation, and specific molecular regulation observed in KRas G12V tumors is consistent with the higher aggressiveness observed in patients with CRC expressing this oncogene.—Alamo, P., Gallardo, A., Di Nicolantonio, F., Pavón, M. A., Casanova, I., Trias, M., Mangues, M. A., Lopez-Pousa, A., Villaverde, A., Vázquez, E., Bardelli, A., Céspedes, M. V., Mangues, R. Higher metastatic efficiency of KRas G12V than KRas G13D in a colorectal cancer model. *FASEB J.* 29, 464–476 (2015). www.fasebj.org**

Key Words: KRas mutants · in vivo *models aggressiveness*

THE HIGH INCIDENCE, poor prognosis, and metastatic spread of CRC make this disease the second most common cause of cancer death in western countries. Forty percent of colorectal tumors bear mutations in the *KRas* gene, the most frequent being the substitution of Gly (KRas WT) by Val (KRas G12V), or Asp, at codon 12 and Gly by Asp at codon 13 (KRas G13D) (1). Most studies investigating the Kras oncogene as a prognostic marker do not differentiate between point mutants and assume all mutants have a similar impact on tumor biology. However, studies in patients with CRC, in animal models and *in vitro*, indicate otherwise.

In CRC, the first studies on the incidence of KRas mutations in codon 12 suggested that different mutations may have a different risk for tumor progression. They

Abbreviations: Angpt2, angiopoietin 2; AAV, adeno-associated virus; CRC, colorectal cancer; CXCR4, C-X-C chemokine receptor type 4; EGFR, epidermal growth factor receptor; EMT, epithelial-mesenchymal transition; FBS, fetal bovine serum; H&E, hematoxylin and eosin; IHC, immunohistochemistry; KRAS, Kirsten rat sarcoma viral oncogene homolog; KRas, protein that in humans is encoded by the *KRas* gene; KRas G13D, Kirsten rat sarcoma viral oncogene homolog with aspartic mutation at codon 13; KRas G12V, Kirsten rat sarcoma viral oncogene homolog with valine mutation at codon 12; KRas WT, KRas wild-type; SDF1α, stromal cell-derived factor 1; uPA/uPAR, urokinase-type plasminogen activator system; VEGFA, vascular endothelial growth factor A

[1] These authors contributed equally to this work.

[2] Correspondence: Biomedical Research Institute Sant Pau (IIB-SantPau), Hospital de la Santa Creu i Sant Pau and CIBER (CIBER-BBN), c/ Sant Antoni Maria Claret, 167, 08025 Barcelona, Spain. E-mail: rmangues@santpau.cat

doi: 10.1096/fj.14-262303

0892-6638/15/0029-0464 © FASEB

found that the prevalence of the different KRas oncoproteins varied among adenomas and among Dukes stage A, B, and C tumors (2). The RASCAL study later established the KRas G12V mutation as the most aggressive KRAS mutation, associating it with a higher risk of recurrence and death in a large cohort of patients with CRC (3–5). This finding was later confirmed in a larger series ($n = 4268$) (3–5). Consistently, KRas G12V mutation confers a metastatic phenotype that renders CRC tumors more aggressive; the incidence of this mutation was found to be higher in primary tumors and metastases of Dukes stage C/D than in stage A/B primary tumors. Moreover, within Dukes stage D cases, KRas G12V mutations were associated with decreased overall survival (2, 6). Distinct Kras oncogene mutations have also shown different transformation capacity in 3T3 fibroblasts *in vitro* (2, 6). In another study, 3T3 transformants that expressed KRas G12C and KRas G13D showed significant differences in their regulation of survival and anchorage-independent growth and in the induction of anoikis in culture (7). It was also shown that these 2 transformants generate different sarcoma tumor types when injected in immunosuppressed mice (8, 9).

The known differences in the transformation capacity *in vitro* and tumorigenicity *in vivo* of different KRas point mutants led us to hypothesize that specific oncogenic KRAS changes could also have different metastatic capacity. The main aim of this study was to compare the metastagenic capacity of 2 SW48 human CRC recombinant clones, expressing KRas G12V or KRas G13D mutants, after their subcutaneous preconditioning followed by orthotopic implantation in the cecum.

MATERIALS AND METHODS

SW48 KRas recombinant clones

The SW48 recombinants expressing heterozygous KRasVal12 (KRas G12V) or KRasAsp13 (KRas G13D) oncogenic mutation were generated by homologous recombination using an adeno-associated-virus (AAV), as previously described (10). The mutations are knocked-in in a heterozygous fashion, and the mutant alleles are therefore expressed under the gene's own promoter. Clones obtained were sequenced to verify the presence of the corresponding KRas point mutation. SW48 control cells bearing the empty vector (KRas WT; KRas proto-oncogene) and the KRas G12V or KRas G13D recombinants clones were cultured in DMEM (ref. 10829018; Invitrogen, Paisley, United Kingdom) supplemented with 10% FBS (ref. F2442; Sigma-Aldrich, St. Louis, MO, USA), 50 U/ml penicillin, and 50 mg/ml streptomycin (re. 15140122; Invitrogen).

Generation of the SW48 metastatic CRC models

We used 5-week-old Swiss female nu/nu mice weighing 18 to 20 g (Charles River Laboratories, L-Arbresle, France) for all *in vivo* experiments. Mice were housed in a sterile environment with bedding, water, and γ-ray-sterilized food *ad libitum*. Experiments were approved by the Animal Ethics Committee at Hospital de la Santa Creu i Sant Pau.

In a preliminary study, we injected the SW48 recombinants expressing KRas G12V or KRas G13D directly into cecum. Due to the low metastatic rate, we used subcutaneous preconditioning before orthotopic injection. This procedure was developed for CRC models and increases the metastatic rate without changing the pattern of metastases (11). This approach provides a sufficient rate of metastasis to compare metastatic development and regulation between KRas G12V- and KRas G13D-derived models.

Briefly, 5 mice were subcutaneously injected with 2×10^7 control SW48 cells or 2×10^7 recombinant cells (KRas G12V or KRas G13D) in DMEM in 2 flanks. Tumors were excised when they reached a volume of 700 mm^3 and disaggregated. A cell suspension (2×10^6 cells resuspended in 50 μl) derived from subcutaneous tumors was injected directly into the mouse cecum wall in control (KRas WT, $n = 9$) and KRas G12V ($n = 11$) and KRas G13D ($n = 7$) mice using the orthotopic cell microinjection procedure (12). Mice were followed once a week and killed when they lost 10% of their body weight or showed signs of pain or illness.

Necropsy and histopathological analysis of primary tumor and metastases

At death, complete necropsy of each animal was performed. We recorded the presence and size of the primary tumor and any visible metastatic foci. Local tumor and the organs with expected metastases (lymph nodes, liver, and lung) were removed, collected, and processed for the histopathological analysis and molecular studies as described previously (12).

Histopathology of primary tumor and all targeted metastatic organs was analyzed by 2 independent observers in samples stained with hematoxylin and eosin (H&E) using 4–20× magnification. We counted the number and area of micro- and macroscopic tumor foci in the affected organs using CellD software, (v3.3), (Olympus). Foci with a diameter of 1 mm or larger and occupying an area $>$ 750,000 mm^2 (13) were considered macroscopic. All smaller foci were considered microscopic.

In primary tumors, we recorded the degree of differentiation and cell morphology, the percentage of tumor necrotic area, the apoptotic and mitotic rate, and the tumor invasion. The apoptotic rates were calculated by counting the number of apoptotic figures in 10 randomly selected 400× field sections stained with H&E. The primary tumor invasive capacity was analyzed as previously described (11). Briefly, after anti-A1/A3 keratin staining, we counted the number of keratin-positive single epithelial tumor cells as well as tumor cell clusters containing 10 or fewer cells (tumor budding) at the primary tumor front. We recorded the number of keratin positive cells or clusters in 3 different tumor fields (400× magnification) for each group.

Molecular analysis of primary tumors and metastatic foci

Molecular analysis was performed using immunohistochemistry (IHC) on formalin-fixed paraffin-embedded tumor tissue. IHC staining was performed using the Dako Autostainer automated Link48 (Dako, Carpinteria, CA, USA) and standard procedures. Samples were incubated with the corresponding primary antibody using the following dilutions: integrins β1, β2, β3, β4, β5, α1, α2, α3, α4, α5, α6, and αv (1:100; ref. ECM440; Chemicon, Atlanta, GA, USA), AKT-p (1:10; ref. M3628, Dako), ANGPT2 (1:50; ref. AP10103b; Abgent, San Diego, CA, USA), MAPK-P (1:100; ref. 4676; Cell Signaling, Danvers, MA, USA), P-MAPK-38 (1:100; ref. 9211S, Cell Signaling Technology, Danvers, MA, USA), vimentin (1:300; ref. M0725, Dako), parathyroid hormonelike hormone (1:50; ref. ABIN394303, Abgent), VEGFA (1:1000; ref. ab46154, Abcam, Cambridge, United Kingdom), β-catenin (1:300; ref. M33539; Dako), Serpine-1 (1:750; ref. ab28207; Abcam), CXCR4 [1:300; Abcam (clone UMB2; #3108-1)], anti-A1/A3 keratin (1:100; ref. M7003; Dako), CD34 (ready to use; ref. IR632; Dako), E-cadherin (1:400; ref. 610182; BD Transduction Laboratories, Franklin Lakes, NJ, USA), which were followed by incubation with mouse or rabbit secondary

antibodies (EndVision; Dako). We next incubated the preparation with 3, 3'-diaminobenzidine substrate (Dako) for 5 min, and contrasted this with hematoxylin. Immunohistochemical slides were evaluated by 2 independent observers who quantified the percentage of stained cells in relation to the total number of tumor cells and their staining intensity (between 0 and 3, where 3 represents the maximum intensity). Finally, the multiplication of both values represented the expression of the protein in each sample.

ELISA assays were performed to determine VEGFA in primary tumor samples extracts following the manufacturer's recommendations (Human VEGFA Platinum ELISA, ref. BMS277/2CE for VEGFA; eBioscience, San Diego, CA, USA).

Statistical analysis

Fisher's exact test was used to analyze possible significant differences between groups in primary tumor or metastatic rates. The Mann-Whitney test was used to compare tumor size, the number of apoptotic or mitotic figures, single tumor cells, and tumor clusters or metastatic foci between groups. Differences in survival between groups were evaluated using Kaplan-Meier curves and the log-rank test. All quantitative values were expressed as mean ± SE, and the statistical tests were performed using SPSS, version 11.0 (IBM, Armonk, NY, USA). Differences between groups were considered significant at $P < 0.05$.

RESULTS

KRas G12V or KRas G13D expression yields higher metastatic rate and aggressiveness than wild-type KRas

Mice bearing KRas G12V or KRas G13D oncogene-expressing tumors had shorter survival than the KRas WT group (190 ± 20 d, $P = 0.04$ for KRas G12V, 188 ± 36 d for KRas G13D, and 265 ± 18 d for KRas WT, $P < 0.001$). The take rate was 33% (3/9) in the KRas WT group, 73% (8/11) in the KRas G12V group, and 57% (4/7) in the KRas G13D group. These differences were not significant (**Table 1**). Mean primary tumor volume at necropsy was significantly higher in both KRas G12V (1201 ± 83 mm^3, $P < 0.05$) and KRas G13D (1395 ± 118 mm^3, $P < 0.01$) groups than in KRas WT mice (964 ± 23 mm^3). Consequently, the KRas mutant groups led to mouse death from intestinal obstruction earlier than in the KRas WT group. All groups developed undifferentiated stage IV tumors, with 40–70% necrosis and a high degree of vascular invasion.

Related to metastatic dissemination, all 3 groups developed lymphatic and lung metastases (**Fig. 1**, Table 1), whereas no liver metastases were recorded in any group. The number of mice developing lymph node metastases was also higher in KRas G12V (73%) and KRas G13D (29%) than in KRas WT (11%) mice. Moreover, there were significantly more lymph node metastatic foci in KRas G12V ($n = 26$) or KRas G13D ($n = 41$) than in KRas WT mice ($P < 0.05$). Similarly, there were more lung metastases in KRas G12V ($n = 34$) and KRas G13D ($n = 27$) than in KRas WT ($n = 10$) mice (Table 1)

KRas G12V showed higher tumor cell survival, invasion, and CXCR4 expressing intravasated tumor emboli than KRas G13D

We analyzed the number of apoptotic and mitotic cells in H&E-stained sections derived from KRas G12V and KRas G13D primary tumors. KRas G12V primary tumors displayed significantly ($P = 0.02$) fewer apoptotic figures per field (7.0 ± 1.2) than KRas G13D tumors (7.4 ± 1.0; **Fig. 2*A*, *B***). Analysis of the mitotic rate showed a trend toward more mitotic figures in KRas G12V (4.9 ± 0.5) than in KRas G13D (2.8 ± 0.4) primary tumors, but it did not reach statistical significance (not shown). In contrast to the observations in primary tumors, the mitotic and apoptotic parameters in KRas G12V and KRas G13D metastatic foci displayed no significant differences between groups (not shown).

We also analyzed the invasion front in the primary tumors. We counted the number of single tumor epithelial cells and the number of tumor buds (Fig. 2*C*, *D*). The number of tumor buds (clusters of 10 or fewer tumor cells) in the primary tumors (white arrows Fig. 2*C*) of the KRas G12V group was significantly ($P = 0.04$) higher than the number of clusters (1.2 ± 0.2/field) in the KRas G13D group (0.6 ± 0.1/field; Fig. 2*D*, *G*). In contrast, the number of single epithelial tumor cells at the invasion front was not significantly different between groups.

Based on the established relationship between the induction of epithelial-mesenchymal transition (EMT) in tumor cells and the acquisition of an increased invasive and metastatic capacities (14), we studied the expression of Snail-1, as a molecular marker of EMT and the expression

TABLE 1. *Number and area of lymph nodes and pulmonary microfoci. macrofoci and visible metastases observed in KRas WT, KRas G12V and KRas G13D SW48 groups*

			Metastatic dissemination*					
			Micro		Macro		Visible	
Metastatic site	SW48 group	Affected animals (n)	Foci (n)	Area mean ± SE ($\times 10^5$ μm^2)	Foci (n)	Area mean ± SE ($\times 10^5$ μm^2)	Foci (n)	Area mean ± SE ($\times 10^5$ μm^2)
Lymph node	KRas WT	1/9*	0	$0^{\ddagger,\S}$	0	0	2	2.486 ± 1754
	KRas G12V	$8/11^{*,\dagger}$	12	$30.3 \pm 8.3^{\ddagger,\P}$	4	$193.2 \pm 28.6^{\|}$	10	$7.523 \pm 1937^{\ddagger}$
	KRas G13D	$2/7^{\dagger}$	27	$12.1 \pm 2.8^{\S,\P}$	1	158.5	13	$2.622 \pm 400^{\ddagger}$
Lung	KRas WT	1/9	10	8.9 ± 0.2	0	0	0	0
	KRas G12V	4/11	34	$6.4 \pm 1.5^{\|}$	0	0	0	0
	KRas G13D	2/7	27	$11.9 \pm 3.8^{\|}$	0	0	0	0

*$P = 0.03$. †$P = 0.08$ (Fisher's test). ‡$P = 0.05$. §$P = 0.028$. ¶$P = 0.02$. ‖$P < 0.001$ (Mann–Whitney test).

of E-cadherin (down-regulated during EMT) and β-catenin (up-regulated during EMT) in the primary tumors, especially at their invasion front, of both groups. We found no differences in Snail-1, E cadherin, and β-catenin expression between KRas G12V and KRas G13D groups (data not shown).

To assess differences in intravasation capacity and CXCR4 expression, we counted the number of tumor emboli inside blood vessels in the tissues adjacent to the primary tumors (Fig. 2) and performed CXCR4 immunostaining. We observed no significant differences in the number of intravasated tumor emboli in the submucosal and pericolic layers of the cecum between groups. The percentage of tumor cells with CXCR4 membrane expression in intravasated tumor emboli of KRas G12V mice (49.8 ± 9.4%) was significantly ($P < 0.001$) higher than in KRas G13D (12.8 ± 4.4%) intravasated tumor emboli (Fig. 2*E, F, H*).

KRas G12V promotes a higher growth rate in lymph node metastases than KRas G13D mice

We analyzed the number of lymphatic and lung metastases, determined their size, and classified them into micro-, macro, and visible metastases. The percentage of mice with lymphatic metastasis was significantly higher in KRas G12V (73%, 8/11) than in KRas G13D (23%, 2/7) mice (Fig. 1, Table 1). Moreover, in KRas G12V mice, the mean area of lymphatic microfoci ($30.3 \pm 8.3 \times 10^4$ μm^2) was significantly ($P = 0.02$) larger than in KRas G13D mice ($12.1 \pm 2.8 \times 10^4$ μm^2). The mean area of the lymphatic macrofoci in KRas G12V mice ($193.2 \pm 28.6 \times 10^4$ μm^2) was also larger than in KRas G13D mice (158.5×10^4 μm^2). Similarly, the mean area of visible lymphatic metastases in KRas G12V mice ($7523 \pm 1937 \times 10^4$ μm^2) was significantly ($P = 0.05$) larger than in KRas G13D mice ($2622 \pm 400 \times 10^4$ μm^2; Fig. 1, Table 1). Thus, as compared with KRas GD13, the expression of the KRas G12V oncogene increased lymph node colonization and increased metastatic foci growth in lymph nodes by promoting the transition from micro- to macrometastases and from macro- to visible metastases. There were no significant differences in the number of mice affected with lung metastasis between KRas G12V and KRas G13D groups. The analysis of metastatic size showed only micrometastasis in KRas G12V or KRas G13D mice. The total number of lung metastases in KRas G12V mice ($n = 34$) was higher than in KRas G13D mice ($n = 27$). The mean size of the lung microfoci was significantly ($P < 0.001$) larger in KRas G13D ($11.9 \pm 3.8 \times 10^4$ μm^2) than in KRas G12V mice ($6.4 \pm 1.5 \times 10^4$ μm^2; Table 1, Fig. 1). No hepatic metastases were observed in SW48-derived KRas WT, KRas G12V, or KRas G13D mice.

KRas G12V and KRas G13D induced different molecular changes in primary tumors

The differences in metastatic dissemination between the KRas G12V and KRas G13D groups triggered the analysis of the expression and/or activation of proteins involved in signaling downstream of KRas (PI3K and MAPK pathways) as well as regulators of survival, adhesion, invasion, and metastatic dissemination to unveil some of the molecular changes that could underlie the observed differences in metastatic dissemination.

KRas G12V primary tumors showed a modestly ($P = 0.05$) higher activation of PI3K pathway than KRas G13D tumors (Fig. 3) as measured by the level of phospho-AKT. Nevertheless, in lymphatic and lung metastasis, there were no significant differences in AKT activation between the KRas G12V and KRas G13D groups. The activation of the Erk pathway, as measured by p-MAPK, showed a trend toward higher activation in KRas G12V *vs.* KRas G13D tumors (data not shown). No significant differences were recorded in the activation of the Erk pathway in lymph node or lung metastasis between KRas G12V and KRas G13D groups (data not shown).

To analyze whether the KRas G12V and KRas G13D oncogenes differentially regulated adhesion, we evaluated the expression of α (1, 2, 3, 4, 5, 6, and ν) and β (1–6) integrins by IHC. Of the 13 evaluated integrins, only β5 and β1 showed a differential expression pattern between groups. The level of β1 integrin expression was significantly ($P = 0.039$) higher in KRas G13D primary tumors than in KRas G12V tumors (**Fig. 4*A, B***). In contrast, the expression of β5 integrin was higher in the KRas G12V primary tumor than in KRas G13D tumors ($P = 0.037$, Fig. 4*G, H*). In addition, the level of β5 or β1 integrin expression was low in both lymph node and lung metastases in the KRas G12V and KRas G13D groups. We did not therefore detect significant differences in the expression of these integrins in metastases between the groups (Fig. 4*C–F, I–L*).

We did not observe expression of CXCR4 in the bulk of primary tumors or their invasive front in KRas G12V and KRas G13D groups. However, CXCR4 was expressed in a subset of cells in metastatic foci involving the lymph nodes, or lung metastasis. The percentage of tumor cells that overexpressed CXCR4 in their membrane in the metastases affecting the lymph nodes in KRas G12V mice was significantly ($P = 0.009$) higher than that in KRas G13D mice (**Fig. 5**). There were no significant differences between groups in CXCR4 expression in lung metastases. We also evaluated the expression of Serpine-1, a regulator of adhesion and invasion. The expression of Serpine-1, as measured by IHC, was significantly ($P = 0.033$) higher in KRas G12V than in KRas G13D primary tumors. These differences in expression were not maintained at the metastatic sites. Thus, no significant differences in Serpine-1 expression in lymphatic metastases were found between KRas G12V and KRas G13D groups. In contrast, the expression of Serpine-1 in lung metastases was significantly ($P < 0.001$) higher in KRas G13D than in KRas G12V mice (Fig. 5).

In primary tumors, the expression of VEGFA measured by ELISA showed significantly higher ($P = 0.025$) levels in KRas G12V than in KRas G13D. We also used IHC to detect VEGFA expression in metastatic foci. We observed no significant differences in lymphatic metastatic foci between groups. In contrast, lung metastases in the KRas G13D group showed a significantly ($P < 0.001$) higher level of VEGFA expression in KRas G13D than in KRas G12V lung metastases (**Fig. 6**). Angpt2 is involved in angiogenesis and metastatic

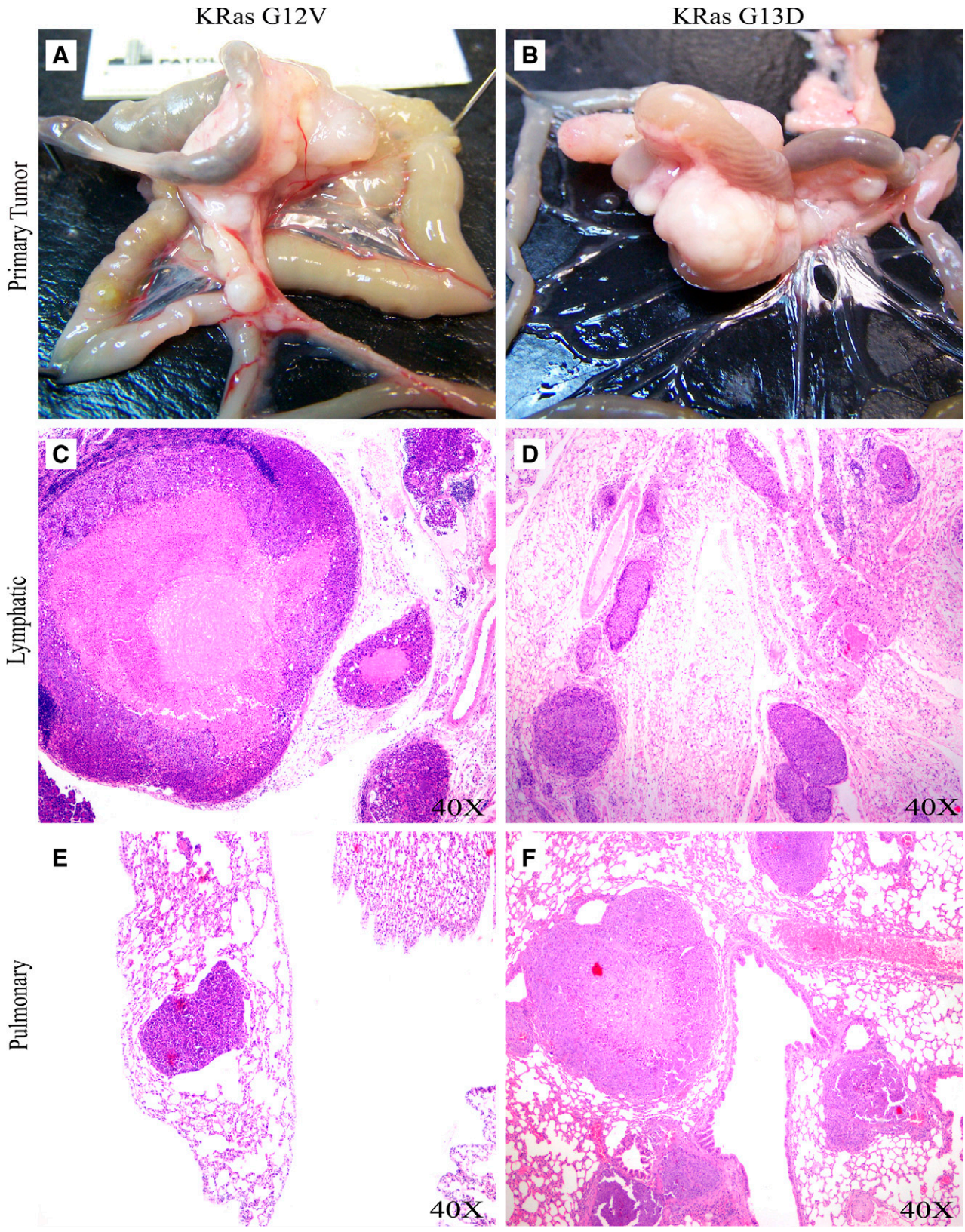

Figure 1. Primary tumor and metastasis development in KRas G12V and KRas G13D mouse models. No differences in primary tumor growth were observed between groups (*A*,*B*). KRas G12V mice developed micro-, macro-, and visible metastasis in the lymph nodes (*C*), which were significantly bigger than the lymph node metastases that developed in KRas G13D mice (*D*). In contrast, KRasG12D and KRas G13D mice developed only microfoci in the lung; however, the lung microfoci in KRas G13D mice were significantly bigger (*F*) than in KRas G12V mice (*E*). The type of metastasis was established as a function of its diameter: microfoci $<$ 1 mm; macrofoci 1–3 mm; visible $>$ 3 mm; H&E staining. Original magnification: $\times$40 (*C*–*F*).

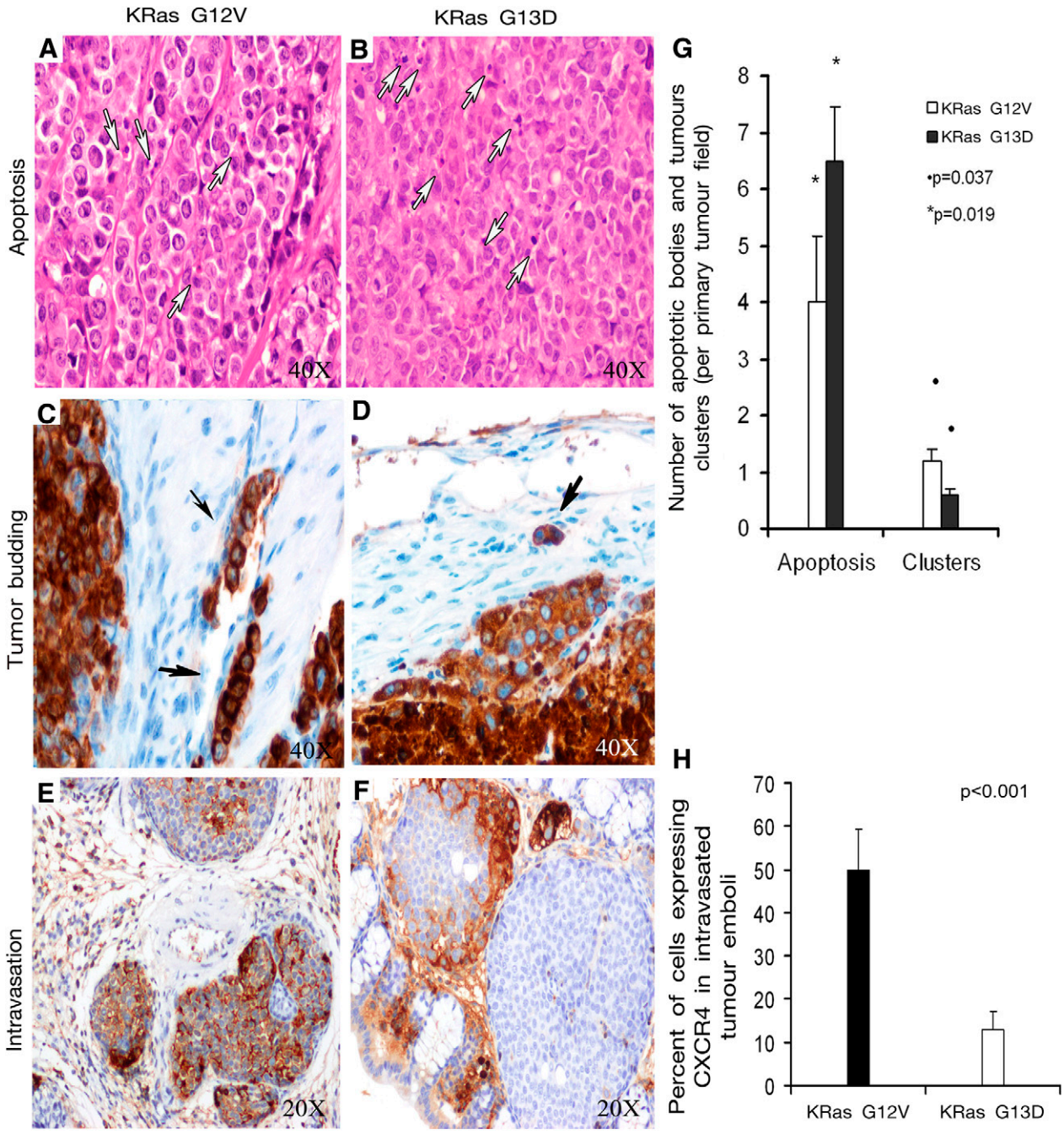

Figure 2. Reduced apoptosis and increased tumor budding and CXCR4-overexpressing intravasated emboli in KRas G12V primary tumors as compared with KRas G13D tumors. Primary tumors in KRas G12V mice (*A*, *G*) showed significantly ($P = 0.019$) fewer apoptotic cells (white arrows) as compared with KRas G13D mice (*B*, *G*). In contrast, primary tumors in KRas G12V mice (*C*) significantly ($P = 0.037$) more pan-keratin-positive tumor clusters (budding) at the invasion front (black arrows) than KRas G13D mice (*D*, *G*). Intravasated tumor emboli in the submucosal and pericolic layers of the cecum had significantly ($P < 0.001$) more cells overexpressing CXCR4 in KRas G12V (*E*, *H*) than in KRas G13D primary tumors (*F*, *H*). Apoptotic bodies, tumor emboli, and tumor buds (clusters of 10 or fewer cells surrounded by stroma at the invasive front) were counted in 10 400× magnified primary tumor fields. Original magnification: ×400 (*A–D*); ×200 (*E–F*).

spread. The analysis of its expression by IHC showed that Angpt2 was significantly ($P = 0.022$) higher in KRas G13D than in KRas G12V primary tumors. The observed differences in Angpt2 expression were also maintained in metastases, because KRas G13D displayed a significantly higher level of this protein in metastatic foci involving lymph nodes ($P = 0.048$) and the lung ($P < 0.001$) than in the KRas G12V group. The level of Angpt2 expression in lymph node metastases that developed in the KRas G13D group was significantly higher ($P = 0.045$) than that observed in KRas G13D primary tumors (Fig. 6).

Subcutaneous SW48 KRas G12V or SW48 KRas G13D tumors used to generate the metastatic orthotopic model

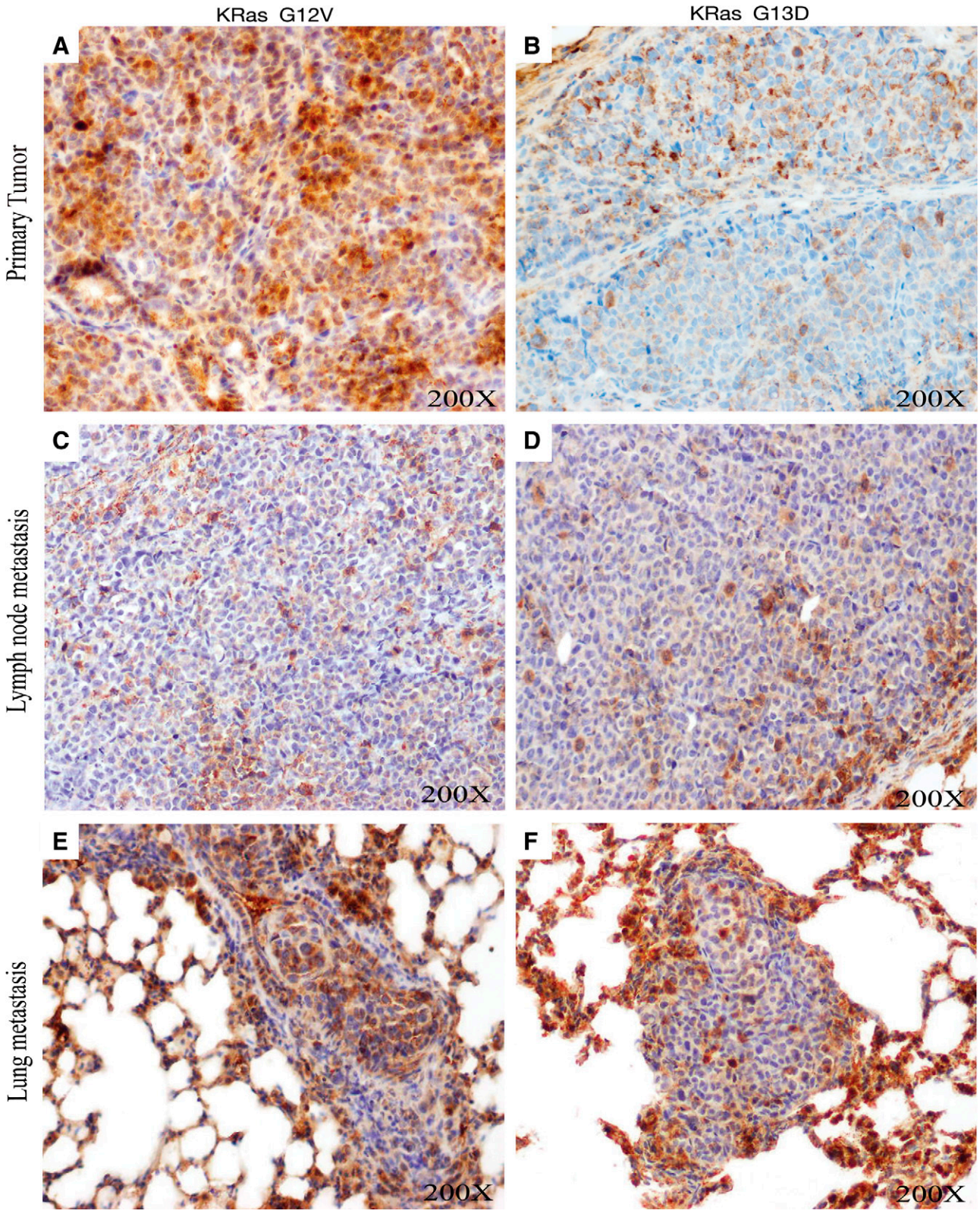

Figure 3. KRas G12V primary tumors showed higher AKT activation than KRas G13D tumors. Primary tumors (*A*) in KRas G12V group showed a significantly ($P < 0.05$) higher level of AKT activation than those (*B*) in the KRas G13D group. No differences in the activation of AKT in lymph node (*C*, *D*) or pulmonary (*E*, *F*) foci were observed between groups (*E*, *F*). Original magnification: ×200 (*A*–*F*).

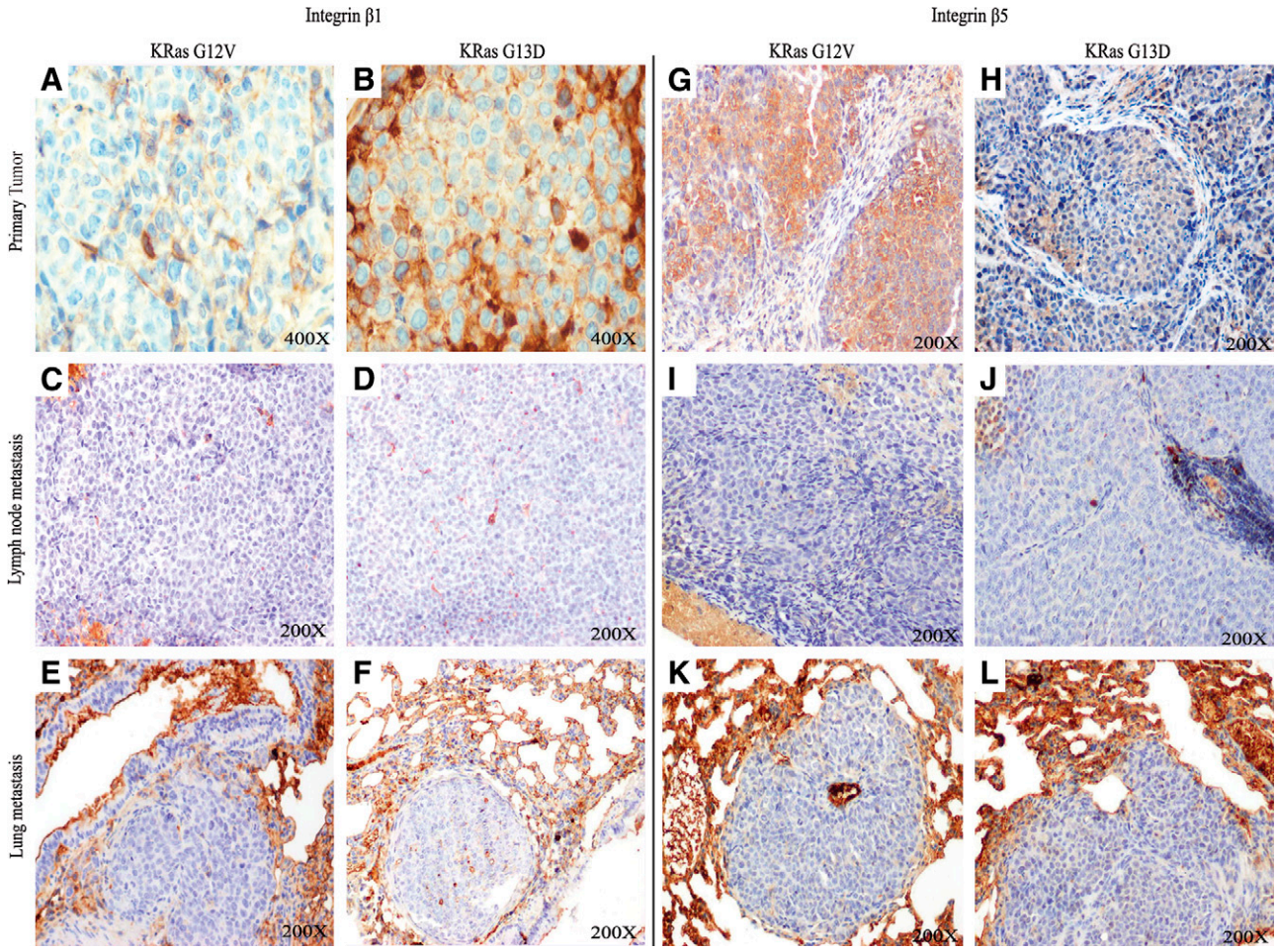

Figure 4. KRas G12V tumors overexpressed integrin $\beta 5$, whereas KRas G13D tumors overexpressed integrin $\beta 1$. Primary tumors (*A*) in KRas G12V group showed significantly lower $\beta 1$ integrin expression than primary tumors (*B*) in the KRas G13D group. No expression of $\beta 1$ integrin was detected in lymph node and pulmonary foci in any group (*C–F*). In contrast, primary tumors (*G*) in KRas G12V group showed significantly higher $\beta 5$ integrin expression than primary tumors (*H*) in the KRas G13D group. No expression of $\beta 5$ integrin was detected in lymph node or pulmonary foci in any group (*I–L*). Original magnification: ×40 (*A, B*); ×200 (*C–L*).

mostly exhibited protein expression levels similar to those found in the derived primary tumors (data not shown). These expression profiles differed from those that we were able to obtain from cell recombinants cultured *in vitro*. Therefore, most molecular changes appear to be induced during their subcutaneous passage.

DISCUSSION

KRas G12V enhances metastases to lymph nodes, an indication of its higher aggressiveness

Our aim was to evaluate whether there were differences in metastatic dissemination between SW48-derived mouse CRC models expressing the KRas G12V or the KRas G13D oncogene. We observed that the KRas G12V mutation increased the percentage of mice with lymph node metastases and the area of lymphatic microfoci, macrofoci, and visible lymph node metastases, as compared with KRas G13D. Therefore, the KRas G12V oncogene increased both the colonization of the lymph nodes and the growth rate of the metastatic foci at this site, promoting the transition from microfoci to large metastases. Our observation of the significantly higher capacity for KRas G12V expressing tumor cells to develop lymphatic metastases suggests higher tumor aggressiveness for this mutation. This argument is consistent with the presence of lymph node metastasis as the strongest predictor of poor prognosis in patients with CRC (15). Moreover, the higher aggressiveness observed in KRas G12V mice is consistent with the shorter overall survival observed in patients with CRC with KRas G12V mutation compared with other Kras mutations in the RASCAL study (3). In human CRC tumors, of 12 different point mutations found at KRas codon 12 or 13, only the KRas G12V mutation conveyed an increased risk of recurrence and death (3, 4). In another study, an analysis restricted only to Dukes stage D patients showed that KRas G12V decreased overall survival as compared with other KRas mutations (6). In our study, we did not detect any difference between KRas G12V and KRas G13D mice regarding the percentage of animals with lung metastases. KRas G13D seems to stimulate the growth of the lung metastasis more than

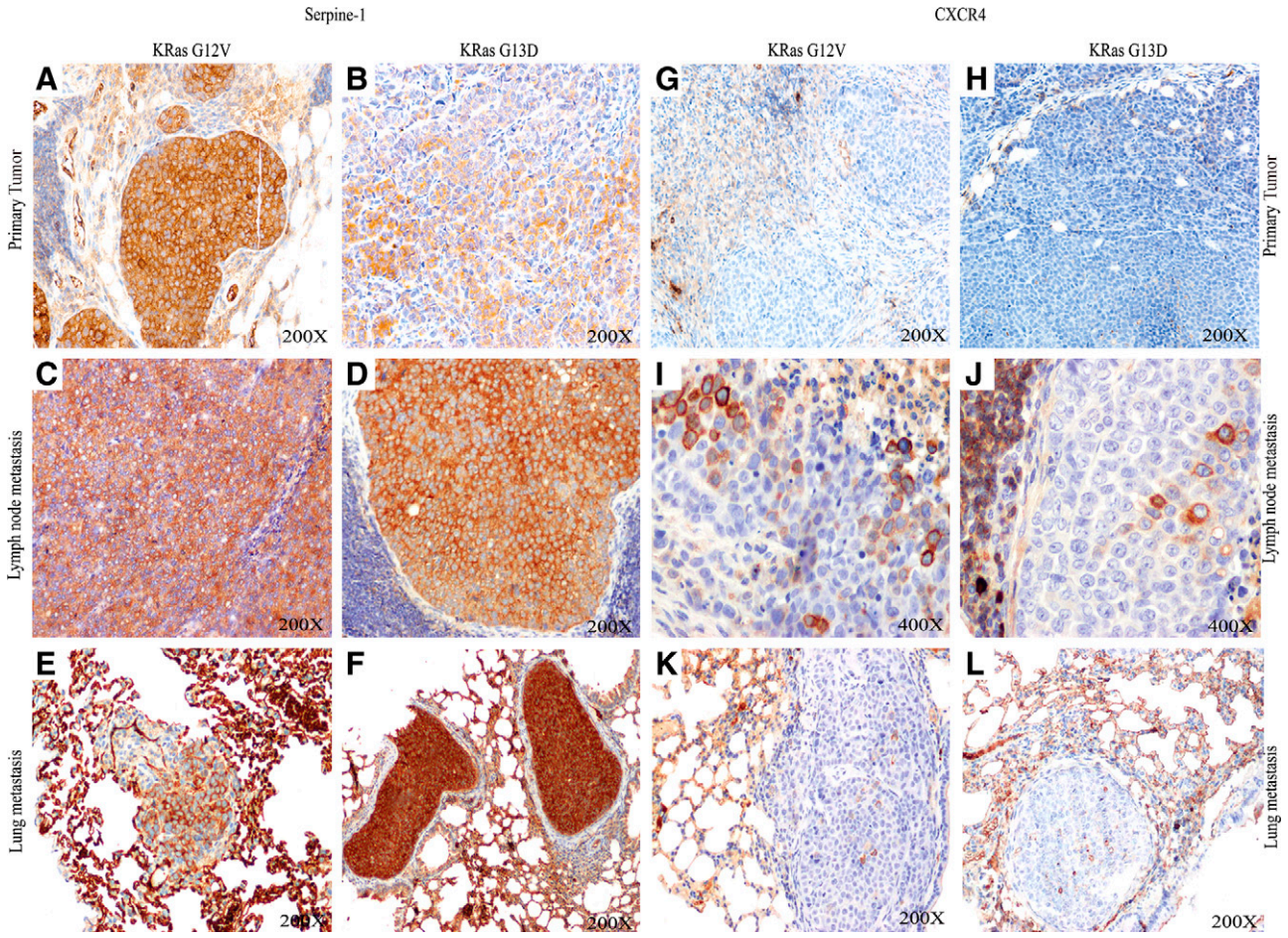

Figure 5. KRas G12V tumors higher levels of Serpine-1 in primary tumors and of CXCR4 in lymph node metastasis, as compared with KRas G13D mice. Primary tumors in KRas G12V mice (*A*) showed significantly higher levels of Serpine-1 expression than primary tumors in KRas G13D mice (*B*). No differences in Serpine-1 expression in lymph node foci were observed between groups (*C*, *D*). In contrast, pulmonary foci in KRas G13D mice showed significantly higher expression of Serpine-1 than in KRas G12V mice (*E*, *F*). Primary tumors in KRAS G12V (*G*) or in KRas G13D (*H*) lacked CXCR4 expression. However, in lymph node metastases, KRas G12V mice showed significantly higher expression of CXCR4 in the membrane than KRas G13D mice (*I*, *J*). Low level of CXCR4 expression in pulmonary foci of KRas G12V (*K*) and KRas G13D (*L*) mice was observed, showing no significant differences between groups. Original magnification: ×200 (*A*–*L*).

KRas G12V, but it does not appear to be able to induce the transition from micro- to macrometastases, because all metastases remained microscopic both in KRas G13D and KRas G12V mice. In liver, we did not observe any metastatic dissemination, because the SW48 CRC cell line does not show an intrinsic ability to metastasize to the liver. We used the SW48 CRC cells because they bear the Kras wild type as well as because they have previously been reported to be amenable to genetic engineering by homologous recombination.

KRas G12V alters protein regulation and induces higher tumor cell survival, invasion, and intravasation

KRas G12V and KRas G13D tumors presented differences in protein expressions involved in invasion, cell survival, and intravasation processes. KRas G12V enhanced cell survival, invasion, and intravasation and overexpressed CXCR4, β5 integrin, VEGFA, and Serpine-1 and over-activated Akt in primary tumors. These alterations may underlie the increased metastatic growth in the lymph nodes found in KRas G12V mice, as compared with KRas G13D. In agreement, the different ras mutants show markedly different transformation capacities (16, 17) and have been associated with different interaction with the downstream effectors (18). In our model, KRas G12V induced activation of the AKT pathway and showed fewer apoptotic markers in comparison with KRas G13D. It has been shown that the Ras Val12 oncogene activates the PI3K/Akt pathway (19, 20), whereas tumors use PKB/Akt pathway activation to inhibit apoptosis, leading to higher migratory, invasive, and metastatic capacities (21, 22). Consistently, we previously showed that the KRas G13D oncogene displays lower transformation capacity in fibroblasts, associated with Akt inactivation and increased apoptosis *in vitro* (7) and *in vivo* (8). Consequently, the KRas G13D oncogene yielded more indolent sarcomas than fibroblasts transformed with the KRas Cysteine 12, the expression of which was associated with Akt activation and less apoptosis. The activation of the Akt pathway has also been observed in stage II patients with CRC where AKT activation predicts tumor recurrence (23).

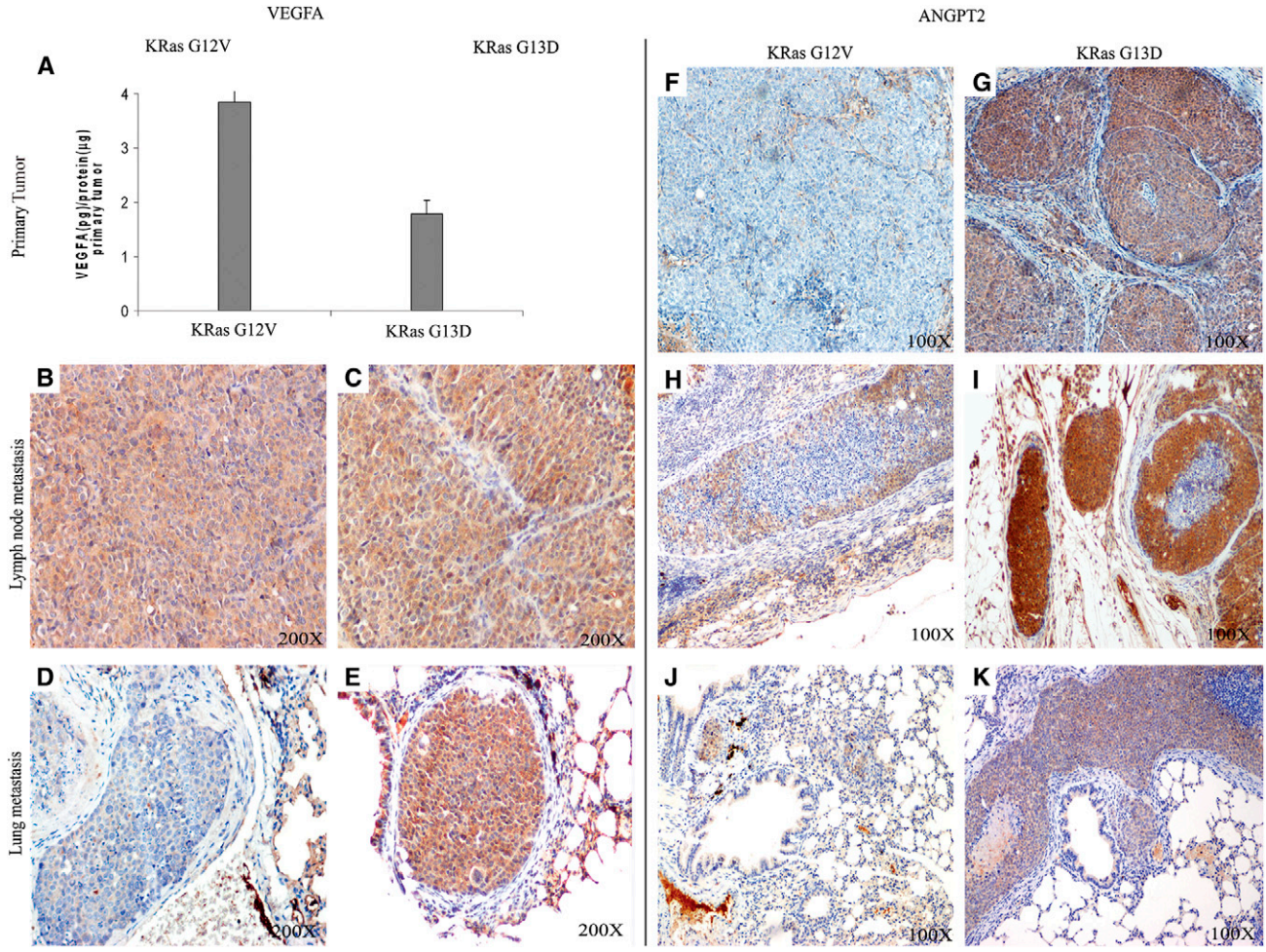

Figure 6. KRas G12V tumors overexpressed VEGFA whereas KRas G13D tumors overexpressed Angpt2. Primary tumors in KRas G12V mice showed significant higher expression of VEGFA than in KRas G13D mice (*A*). In contrast, no differences in the VEGFA expression in lymph node foci were observed between groups (*B,C*), whereas in pulmonary foci the expression of VEGFA was significantly lower in KRas G12V (*D*) than in KRas G13D (*E*) mice. KRas G12V primary tumors (*F*) showed significantly lower levels of Angpt2 expression than KRas G13D tumors (*G*). Similarly, lymph node (*H, I*) or pulmonary (*J, K*) metastasis in KRas G13D mice showed significantly higher Angpt2 expression than KRas G12V mice. Original magnification: ×200 (*C–F*); ×100 (*G–K*).

We also observed that KRas G12V enhanced budding in primary tumors associated with enhanced lymph node metastases. In agreement with this finding, in patients with CRC, tumor budding at the invasive front is associated with lymph node metastases and poor prognosis (24–28).

The increased invasion observed in KRAS mutant tumors could be caused by several distinct molecular mechanisms. We discarded EMT as responsible for the enhanced metastases observed in KRas G12V because we did not observe differences in single cell count or in Snail-1, E-cadherin, or β-catenin expression between KRas G12V and KRas G13D tumors at the invasive front, characteristic of EMT (14). Nevertheless, in CRC models, several reports support higher migratory and metastatic capacity for tumors that overexpress β5 integrin together with Akt activation (observed in our KRas G12V tumors) compared with tumors with β1 expression and Akt inactivation (observed in KRas G13D tumors). Similarly, migration of the SW480 CRC cell line (which expresses KRas G12V) in type I collagen is dependent on αvβ5 expression and Akt activation (29). In contrast, down-regulation of αvβ5 integrin in this model leads to α2β1-dependent and Akt-independent migration, supporting a cross-regulation between β5 and β1 associated with differential Akt regulation (29). Moreover, αvβ5-dependent migration on vitronectin has been associated with enhanced liver metastases in the LM-LM6 CRC model, whereas Akt inactivation blocked this migration (30). Consistently, the KRas G12V oncogene mutation induces β5 expression and blocks integrin β1 expression in colon epithelial cells (31).

Serpine-1 is also overexpressed in KRas G12V tumors and may contribute to their enhanced invasiveness and metastases. Thus, in patients with CRC, Serpine-1 overexpression in primary tumors is associated with lymph node metastasis (32), whereas high levels of Serpine-1 in plasma is a marker of poor prognosis (33). In addition, cross-talk between β5 and β1, like that described in CRC models, has been reported in fibroblasts, in which integrin β5 degradation leading to β1 up-regulation is controlled by urokinase-type plasminogen activator system (uPA/uPAR) system activation (34). This system is inactivated by serpine-1.

This suggests that Serpine-1, a protein overexpressed together with β5 integrin in KRas G12V tumors, may regulate this crosstalk in our CRC model, when serpine-1 covalently binds to and inactivates the uPA/uPAR system.

In KRas G12V mice, we observed an increased percentage of CXCR4-overexpressing cells in intravasated tumor emboli in the submucosal and pericolic layers of the cecum. We also found more CXCR4 cells in lymph node metastases. These findings suggest the CXCR4 receptor plays a role in intravasation, enhancing lymph node metastases in our model. This suggestion is in agreement with the association between intravasated tumor emboli (35) and lymphovascular invasion (36) with lymph node metastasis and poor prognosis in patients with CRC. Similarly, CXCR4 overexpression in primary tumors increased the risk of recurrence and poor survival (37) in patients with CRC. Moreover, expression of CXCR4 in the HT29 CRC model favors tumor cell extravasation (38), whereas CXCR4 expression promotes the growth of CT-26 CRC micrometastases in the colonized organ (39). In addition, CXCR4 + HT29 CRC cells are capable of establishing a paracrine signaling with stromal cell-derived factor 1 (SDF1α) secreting lymph node stromal cells (40), which may drive their dissemination toward this metastatic site. Similarly, CXCR4-expressing tumor cells are able to migrate through hypoxic SDF1α, secreting endothelial cells (transendothelial migration), and invade blood vessels in a breast cancer model (41).

In agreement with enhanced VEGFA tumor expression and lymph node metastases observed in KRas G12V mice, VEGFA and CXCR4 are associated with lymph node metastasis and poor prognosis in patients with CRC (42–44). Similarly, in the CT26 CRC model, VEGFA induces angiogenesis and promotes vascular permeability, leading to metastatic spread (45, 46). Finally, and in contrast with the reports on KRas G12V-disregulated proteins, no publications on the prognostic value in patients with CRC have been reported for the proteins overexpressed in KRas G13D tumors (integrin β1 or Angpt2).

Differential protein regulation in KRas G12V and KRas G13D mice between primary tumors and metastases

Whereas protein expression in primary tumors may contribute to determine the mechanism of invasion and intravasation, such expression in metastases may indicate the pathway used for metastatic foci growth at the metastatic site. In our model, KRas G13D tumors overexpressed Angpt2 and developed larger lung micrometastasis than with KRas G12V. In this regard, Angpt2 expression in the primary tumor may have promoted colonization of the lung, because it enhances cancer cell extravasation by loosening the endothelial cell junctions, leading to increased metastasis in the lung (47, 48). In contrast, the high levels of Angpt2 observed in lung microfoci in KRas G13D mice may have determined the inability of these tumor cells to promote vascularization. It has been observed that high levels of Angpt2 induce microvessel regression and inhibit tumor growth in the HT29 subcutaneous CRC model (49).

The oncogene expressed in primary tumors (KRas G12V or KRas G13D) may determine the pattern of protein expression. Interestingly, the pattern of protein expression we found in orthotopic primary tumors was already present in the subcutaneous tumors used for KRas G12V and KRas G13D preconditioning. Thus, both orthotopic and subcutaneous tumors that expressed KRas G12V showed higher Akt activation and integrin β5 overexpression than KRas G13D. However, the environment in the site where the tumor grows may also contribute to regulate protein expression in tumor cells. In contrast with our observations in primary tumors, the number of mitotic and apoptotic figures in KRas G12V and KRas G13D metastatic foci did not differ significantly between groups. Therefore, different metastatic organs appear to regulate apoptosis in a different way. We also observed that the pattern of protein expression in metastases differed greatly from the corresponding pattern in the primary tumor. This suggests that that the tumor environment also contributes to determining this pattern. In support of this suggestion, we observed that VEGFA or Serpine-1 was overexpressed in KRas G12V but not in KRas G13D primary tumors. In lung metastases, these 2 proteins were overexpressed in KRas G13D compared with KRas G12V mice.

Clinical implications

In summary, this is the first report to describe a different metastatic capacity and a pattern of protein expression for distinct KRas point mutations in an orthotopic mouse CRC model, as well as an association between metastatic capacity and CXCR4-overexpressing tumor emboli. Our results highlight the need to consider the different KRas mutants as separate entities.

These results are consistent with the higher aggressiveness of KRas G12V mutation observed in patients with CRC, as compared with any other KRas mutation, and support the notion that different KRas mutants may associate with different prognosis. The different regulation of cell survival and Akt-p between KRas G12V and KRas G13D in our model may also indicate different responses between KRas G12V and KRas G13D to antitumor drugs. This is in agreement with the reported lack of Akt activation by KRas G13D (7, 8) and with the higher sensitivity of KRas G13D CRC cells, as compared with KRas G12V to the epidermal growth factor receptor (EGFR) inhibitor cetuximab *in vitro* and longer overall survival in KRas G13D patients compared with other KRas mutations when being treated with the EGFR inhibitor cetuximab (50). However, more recent clinical data are contradictory (51). Future studies should explore other KRas mutations with lower transforming capacity in relation to their ability to engage different pathway effectors, their propensity to metastasize, as well as their impact on anticancer treatments. FJ

The authors thank Carmen Cabrera for technical support and Carolyn Newey for revising the English text. They

acknowledge performing animal work in the CIBER-BBN Nanotoxicology unit. R.M. acknowledges funding from Instituto de Salud Carlos III (grant PI12/01861), la Fundació La Marató de TV3 416/C/2013-2030 CIBER-BBN NanoMets project, and AGAUR (2009-SGR1437). F.D.N. and A.B. are coinventors on a patent describing the process of making isogenic cell lines. A. B. is a shareholder of Horizon Discovery, a company exploiting AAV-mediated genome editing to create isogenic cell lines and to which the SW48 cells described in this study have been licensed for commercial use. P.A. designed and performed the experiments, analyzed the data and participated in text writing. A.G. carried out the histopathological analysis of mouse samples. F.D. performed the KRas homologous recombination experiments. I.C. and M.A.P. performed the experiments and the statistical analyses of mice data. M.T. and M.A.M. analyzed data. E.V., A.V., F.D., and A.B. participated in the discussion of data and text writing. R.M. and M.V.C. contributed equally to this study and they conceived the project, analyzed data, supervised the overall project, and wrote the manuscript. The authors declare no conflicts of interest.

REFERENCES

1. Barbacid, M. (1987) ras genes. *Annu. Rev. Biochem.* **56**, 779–827
2. Moerkerk, P., Arends, J. W., van Driel, M., de Bruïne, A., de Goeij, A., and ten Kate, J. (1994) Type and number of Ki-ras point mutations relate to stage of human colorectal cancer. *Cancer Res.* **54**, 3376–3378
3. Andreyev, H. J., Norman, A. R., Cunningham, D., Oates, J. R., and Clarke, P. A. (1998) Kirsten ras mutations in patients with colorectal cancer: the multicenter "RASCAL" study. *J. Natl. Cancer Inst.* **90**, 675–684
4. Andreyev, H. J., Norman, A. R., Cunningham, D., Oates, J., Dix, B. R., Iacopetta, B. J., Young, J., Walsh, T., Ward, R., Hawkins, N., et al. (2001) Kirsten ras mutations in patients with colorectal cancer: the 'RASCAL II' study. *Br. J. Cancer* **85**, 692–696
5. Span, M., Moerkerk, P. T., De Goeij, A. F., and Arends, J. W. (1996) A detailed analysis of K-ras point mutations in relation to tumor progression and survival in colorectal cancer patients. *Int. J. Cancer* **69**, 241–245
6. Al-Mulla, F., Going, J. J., Sowden, E. T., Winter, A., Pickford, I. R., and Birnie, G. D. (1998) Heterogeneity of mutant versus wild-type Ki-ras in primary and metastatic colorectal carcinomas, and association of codon-12 valine with early mortality. *J. Pathol.* **185**, 130–138
7. Guerrero, S., Casanova, I., Farré, L., Mazo, A., Capellà, G., and Mangues, R. (2000) K-ras codon 12 mutation induces higher level of resistance to apoptosis and predisposition to anchorage-independent growth than codon 13 mutation or proto-oncogene overexpression. *Cancer Res.* **60**, 6750–6756
8. Guerrero, S., Figueras, A., Casanova, I., Farré, L., Lloveras, B., Capellà, G., Trias, M., and Mangues, R. (2002) Codon 12 and codon 13 mutations at the K-ras gene induce different soft tissue sarcoma types in nude mice. *FASEB J.* **16**, 1642–1644
9. Céspedes, M. V., Casanova, I., Parreño, M., and Mangues, R. (2006) Mouse models in oncogenesis and cancer therapy. *Clin. Transl. Oncol.* **8**, 318–329
10. Di Nicolantonio, F., Arena, S., Gallicchio, M., Zecchin, D., Martini, M., Flonta, S. E., Stella, G. M., Lamba, S., Cancelliere, C., Russo, M., et al. (2008) Replacement of normal with mutant alleles in the genome of normal human cells unveils mutation-specific drug responses. *Proc. Natl. Acad. Sci. USA* **105**, 20864–20869
11. Alamo, P., Gallardo, A., Pavón, M. A., Casanova, I., Trias, M., Mangues, M. A., Vázquez, E., Villaverde, A., Mangues, R., and Céspedes, M. V. (2014) Subcutaneous preconditioning increases invasion and metastatic dissemination in mouse colorectal cancer models. *Dis. Model. Mech.* **7**, 387–396
12. Céspedes, M. V., Espina, C., García-Cabezas, M. A., Trias, M., Boluda, A., Gómez del Pulgar, M. T., Sancho, F. J., Nistal, M., Lacal, J. C., and Mangues, R. (2007) Orthotopic microinjection of human colon cancer cells in nude mice induces tumor foci in all clinically relevant metastatic sites. *Am. J. Pathol.* **170**, 1077–1085
13. Folkman, J. (1983) Angiogenesis: initiation and modulation. *Symp. Fundam. Cancer Res.* **36**, 201–208
14. Yang, J. and Weinberg, R.A. (2008) Epithelial-mesenchymal transition: at the crossroads of development and tumor metastasis. *Dev. Cell* **14**, 818–829
15. Resch, A., and Langner, C. (2013) Lymph node staging in colorectal cancer: old controversies and recent advances. *World J. Gastroenterol.* **19**, 8515–8526
16. Fasano, O., Aldrich, T., Tamanoi, F., Taparowsky, E., Furth, M., and Wigler, M. (1984) Analysis of the transforming potential of the human H-ras gene by random mutagenesis. *Proc. Natl. Acad. Sci. USA* **81**, 4008–4012
17. Seeburg, P. H., Colby, W. W., Capon, D. J., Goeddel, D. V., and Levinson, A. D. (1984) Biological properties of human c-Ha-ras1 genes mutated at codon 12. *Nature* **312**, 71–75
18. Downward, J. (2003) Targeting RAS signalling pathways in cancer therapy. *Nat. Rev. Cancer* **3**, 11–22
19. Monaco, R., Chen, J. M., Friedman, F. K., Brandt-Rauf, P., Chung, D., and Pincus, M. R. (1995) Structural effects of the binding of GTP to the wild-type and oncogenic forms of the ras-gene-encoded p21 proteins. *J. Protein Chem.* **14**, 721–729
20. Pacold, M. E., Suire, S., Perisic, O., Lara-Gonzalez, S., Davis, C. T., Walker, E. H., Hawkins, P. T., Stephens, L., Eccleston, J. F., and Williams, R. L. (2000) Crystal structure and functional analysis of Ras binding to its effector phosphoinositide 3-kinase gamma. *Cell* **103**, 931–943
21. Vivanco, I., and Sawyers, C. L. (2002) The phosphatidylinositol 3-Kinase AKT pathway in human cancer. *Nat. Rev. Cancer* **2**, 489–501
22. Xue, G., and Hemmings, B. A. (2013) PKB/Akt-dependent regulation of cell motility. *J. Natl. Cancer Inst.* **105**, 393–404
23. Malinowsky, K., Nitsche, U., Janssen, K. P., Bader, F. G., Späth, C., Drecoll, E., Keller, G., Höfler, H., Slotta-Huspenina, J., and Becker, K. F. (2014) Activation of the PI3K/AKT pathway correlates with prognosis in stage II colon cancer. *Br. J. Cancer* **110**, 2081–2089
24. Mitrovic, B., Schaeffer, D. F., Riddell, R. H., and Kirsch, R. (2012) Tumor budding in colorectal carcinoma: time to take notice. *Mod. Pathol.* **25**, 1315–1325
25. Zlobec, I., Hädrich, M., Dawson, H., Koelzer, V. H., Borner, M., Mallaev, M., Schnüriger, B., Inderbitzin, D., and Lugli, A. (2014) Intratumoural budding (ITB) in preoperative biopsies predicts the presence of lymph node and distant metastases in colon and rectal cancer patients. *Br. J. Cancer* **110**, 1008–1013
26. Kazama, S., Watanabe, T., Ajioka, Y., Kanazawa, T., and Nagawa, H. (2006) Tumour budding at the deepest invasive margin correlates with lymph node metastasis in submucosal colorectal cancer detected by anticytokeratin antibody CAM5.2. *Br. J. Cancer* **94**, 293–298
27. Kye, B. H., Jung, J. H., Kim, H. J., Kang, S. G., Cho, H. M., and Kim, J. G. (2012) Tumor budding as a risk factor of lymph node metastasis in submucosal invasive T1 colorectal carcinoma: a retrospective study. *BMC Surg.* **12**, 16
28. Giger, O. T., Comtesse, S. C., Lugli, A., Zlobec, I., and Kurrer, M. O. (2012) Intra-tumoral budding in preoperative biopsy specimens predicts lymph node and distant metastasis in patients with colorectal cancer. *Mod. Pathol.* **25**, 1048–1053
29. Defilles, C., Lissitzky, J. C., Montero, M. P., André, F., Prévot, C., Delamarre, E., Marrakchi, N., Luis, J., and Rigot, V. (2009) alphavbeta5/beta6 integrin suppression leads to a stimulation of alpha2beta1 dependent cell migration resistant to PI3K/Akt inhibition. *Exp. Cell Res.* **315**, 1840–1849
30. Yoshioka, T., Nishikawa, Y., Ito, R., Kawamata, M., Doi, Y., Yamamoto, Y., Yoshida, M., Omori, Y., Kotanagi, H., Masuko, T., and Enomoto, K. (2010) Significance of integrin $\alpha v\beta 5$ and erbB3 in enhanced cell migration and liver metastasis of colon carcinomas stimulated by hepatocyte-derived heregulin. *Cancer Sci.* **101**, 2011–2018
31. Yan, Z., Chen, M., Perucho, M., and Friedman, E. (1997) Oncogenic Ki-ras but not oncogenic Ha-ras blocks integrin beta1-chain maturation in colon epithelial cells. *J. Biol. Chem.* **272**, 30928–30936
32. Sakakibara, T., Hibi, K., Koike, M., Fujiwara, M., Kodera, Y., Ito, K., and Nakao, A. (2005) Plasminogen activator inhibitor-1 as a potential marker for the malignancy of colorectal cancer. *Br. J. Cancer* **93**, 799–803
33. Nielsen, H. J., Pappot, H., Christensen, I. J., Brünner, N., Thorlacius-Ussing, O., Moesgaard, F., Danø, K., and Grøndahl-Hansen, J. (1998)

Association between plasma concentrations of plasminogen activator inhibitor-1 and survival in patients with colorectal cancer. *BMJ* **316**, 829–830
34. Lee, C.C. and Huang, T.S. (2005) Plasminogen activator inhibitor-1: the expression, biological functions, and effects on tumorigenesis and tumor cell adhesion and migration. *J. Cancer Molecules* **1**, 26–35
35. Son, H. J., Song, S. Y., Lee, W. Y., Yang, S. S., Park, S. H., Yang, M. H., Yoon, S. H., and Chun, H. K. (2008) Characteristics of early colorectal carcinoma with lymph node metastatic disease. *Hepatogastroenterology* **55**, 1293–1297
36. Lim, S. B., Yu, C. S., Jang, S. J., Kim, T. W., Kim, J. H., and Kim, J. C. (2010) Prognostic significance of lymphovascular invasion in sporadic colorectal cancer. *Dis. Colon Rectum* **53**, 377–384
37. Kim, J., Takeuchi, H., Lam, S. T., Turner, R. R., Wang, H. J., Kuo, C., Foshag, L., Bilchik, A. J., and Hoon, D. S. (2005) Chemokine receptor CXCR4 expression in colorectal cancer patients increases the risk for recurrence and for poor survival. *J. Clin. Oncol.* **23**, 2744–2753
38. Gassmann, P., Haier, J., Schlüter, K., Domikowsky, B., Wendel, C., Wiesner, U., Kubitza, R., Engers, R., Schneider, S. W., Homey, B., and Müller, A. (2009) CXCR4 regulates the early extravasation of metastatic tumor cells in vivo. *Neoplasia* **11**, 651–661
39. Zeelenberg, I. S., Ruuls-Van Stalle, L., and Roos, E. (2003) The chemokine receptor CXCR4 is required for outgrowth of colon carcinoma micrometastases. *Cancer Res.* **63**, 3833–3839
40. Margolin, D. A., Silinsky, J., Grimes, C., Spencer, N., Aycock, M., Green, H., Cordova, J., Davis, N. K., Driscoll, T., and Li, L. (2011) Lymph node stromal cells enhance drug-resistant colon cancer cell tumor formation through SDF-1α/CXCR4 paracrine signaling. *Neoplasia* **13**, 874–886
41. Jin, F., Brockmeier, U., Otterbach, F., and Metzen, E. (2012) New insight into the SDF-1/CXCR4 axis in a breast carcinoma model: hypoxia-induced endothelial SDF-1 and tumor cell CXCR4 are required for tumor cell intravasation. *Mol. Cancer Res.* **10**, 1021–1031
42. Fukunaga, S., Maeda, K., Noda, E., Inoue, T., Wada, K., and Hirakawa, K. (2006) Association between expression of vascular endothelial growth factor C, chemokine receptor CXCR4 and lymph node metastasis in colorectal cancer. *Oncology* **71**, 204–211
43. George, M. L., Tutton, M. G., Janssen, F., Arnaout, A., Abulafi, A. M., Eccles, S. A., and Swift, R. I. (2001) VEGF-A, VEGF-C, and VEGF-D in colorectal cancer progression. *Neoplasia* **3**, 420–427
44. Ottaiano, A., Franco, R., Aiello Talamanca, A., Liguori, G., Tatangelo, F., Delrio, P., Nasti, G., Barletta, E., Facchini, G., Daniele, B., Di Blasi, A., Napolitano, M., Ieranò, C., Calemma, R., Leonardi, E., Albino, V., De Angelis, V., Falanga, M., Boccia, V., Capuozzo, M., Parisi, V., Botti, G., Castello, G., Vincenzo Iaffaioli, R., and Scala, S. (2006) Overexpression of both CXC chemokine receptor 4 and vascular endothelial growth factor proteins predicts early distant relapse in stage II-III colorectal cancer patients. *Clin. Cancer Res.* **12**, 2795–2803
45. Criscuoli, M. L., Nguyen, M., and Eliceiri, B. P. (2005) Tumor metastasis but not tumor growth is dependent on Src-mediated vascular permeability. *Blood* **105**, 1508–1514
46. Weis, S., Cui, J., Barnes, L., and Cheresh, D. (2004) Endothelial barrier disruption by VEGF-mediated Src activity potentiates tumor cell extravasation and metastasis. *J. Cell Biol.* **167**, 223–229
47. Minami, T., Jiang, S., Schadler, K., Suehiro, J., Osawa, T., Oike, Y., Miura, M., Naito, M., Kodama, T., and Ryeom, S. (2013) The calcineurin-NFAT-angiopoietin-2 signaling axis in lung endothelium is critical for the establishment of lung metastases. *Cell Reports* **4**, 709–723
48. Rigamonti, N., and De Palma, M. (2013) A role for angiopoietin-2 in organ-specific metastasis. *Cell Rep.* **4**, 621–623
49. Cao, Y., Sonveaux, P., Liu, S., Zhao, Y., Mi, J., Clary, B. M., Li, C. Y., Kontos, C. D., and Dewhirst, M. W. (2007) Systemic overexpression of angiopoietin-2 promotes tumor microvessel regression and inhibits angiogenesis and tumor growth. *Cancer Res.* **67**, 3835–3844
50. De Roock, W., Jonker, D. J., Di Nicolantonio, F., Sartore-Bianchi, A., Tu, D., Siena, S., Lamba, S., Arena, S., Frattini, M., Piessevaux, H., Van Cutsem, E., O'Callaghan, C. J., Khambata-Ford, S., Zalcberg, J. R., Simes, J., Karapetis, C. S., Bardelli, A., and Tejpar, S. (2010) Association of KRAS p.G13D mutation with outcome in patients with chemotherapy-refractory metastatic colorectal cancer treated with cetuximab. *JAMA* **304**, 1812–1820
51. Peeters, M., Douillard, J. Y., Van Cutsem, E., Siena, S., Zhang, K., Williams, R., and Wiezorek, J. (2013) Mutant KRAS codon 12 and 13 alleles in patients with metastatic colorectal cancer: assessment as prognostic and predictive biomarkers of response to panitumumab. *J. Clin. Oncol.* **31**, 759–765

Received for publication August 18, 2014.
Accepted for publication September 19, 2014.